

TIM: Tree Imaging Machine for low-cost digital images of tree cores and cookies

Your Name

March 3, 2025

Abstract

Studies of tree rings (dendrochronology) have benefitted recently from new methods to image wood rapidly and efficiently, helping to scale up the number and quality of image samples. Current open-source approaches are, however, limited in dimensionality and can be cost-prohibitive. The Tree Imaging Machine (TIM) is a do-it-yourself scanning tool made to digitize tree cookies and cores that address these limitations. TIM takes partially overlapping microscopic images of samples and stitches the individual images together to form a mosaic, which can be zoomed in to visualize features on the scale of 0.01 mm. With scans of up to 21 140 DPI, TIM produces one of the highest resolution images among similar tools for the competitive price of less than \$3 000 USD. We designed TIM to have a large working plane to allow digitizing cores over 50 cm and complete cookies. Operators can prepare sample batches of multiple cores and cookies, letting the machine work until the queue is finished. All of the 3D printed parts are available for download on the [NIH 3D printing repository](<https://doi.org/10.60705/3DPX/21561.3>) and the software is open source, with instructions to recreate this tool available on [GitHub](<https://github.com/temporalecologylab/TreeRings>). TIM provides an important advance in scanning resolution, tree cookie sampling, maximum core sample size, batch digitization, and cost in a single package. This promotes the digitization of larger samples and can collect data at finer resolutions in an open-source design which can be built on and improved as new technologies become available.

1 Introduction

Incremental growth rings from trees provide a valuable proxy record of the environment and climate. They have proven to provide the highest accuracy, precision, and reliable dating among alternatives [10]. Multiple fields—from climatology to forestry and ecology—rely on tree rings to understand how the environment affects tree growth. Tree rings have been critical to reconstructing past climates of regional and local environments, informing our understanding of climate change today [3] [21] [7] [19]. They are also increasingly used in ecology, to understand how plant competition affects tree growth in addition to climate [1] and have implications in forestry to managing stand dynamics [2]. As tree growth and forest management becomes more critical to mitigating climate change, scaling up the collection and processing of tree ring samples has become increasingly important.

Two types of tree sampling techniques are used to capture the variation of tree rings. The first sample type is collected using an incremental borer, used to remove a cylindrical core from a tree. The second sample type is an entire cross section of a tree, often called a tree cookie. Tree cookies present an opportunity to measure as many radii from the sample as desired [20]. Measuring the width between incremental rings from tree samples is first step towards gaining insights.

The first computer based method to measure tree ring widths used a microcomputer, a stage micrometer, and a push button. A trained technician shifted a core underneath a microscope objective and pushed a button connected to a microcomputer to record a ring's location [18]. This method was high precision but depended heavily on specific technicians and maintained no image record [8].

Image analysis of tree rings was later implemented to reduce both errors in sampling and sampling bias across individual technicians, with major methods developed in the 1980s and 1990s to digitize tree ring samples using optical scanning [11] [6]. Optical scanners are still readily available for purchase, using a top of the line scanner, like the Epson Perfection V850 Pro produces maximum resolutions of 6 400 dpi and scan an area of up to 21.6 cm x 29.7 cm. More recent techniques have aimed to achieve higher resolutions and/or larger samples through a different digitization approach. Samples are digitized using an image-capturing system built using a microscope camera to take images, motors to move the sample or camera, a computer to manage the capturing, and a second, more powerful, computer to stitch images into a larger composite image. Decreasing the field of view of each captured image increases the resolution of the final stitched image without restricting the size of the sample [14]. Stitching multiple images into one mosaic is a common technique used in other fields such as mineralogy and cellular biology [17, 13]. The first implementation of the capture and stitch method was the Advanced Tree-Ring Image Capturing System (ATRICS) [8].

Since ATRICS was introduced in 2007, image capture and stitching of tree rings has become more common. Today CaptuRING offers a more modern do-it-yourself alternative to ATRICS, creating scans up to 5 339 dpi using a DSLR camera and motorized stage [4]. Another alternative, Gigapixel, achieves an impressive 19 812 dpi with the same DSLR image capture and composite stitch method [5]. While CaptuRING and Gigapixel both use DSLR cameras and motorized movement, they differ on two fronts. First, Gigapixel's camera is traversed across a stationary sample while CaptuRING moves a core sample underneath a stationary camera. With a mobile camera, multiple samples can be recorded sequentially without needing to remove a sample from a stage upon image completion—significantly reducing the active setup time for an operator. Second, Gigapixel automatically stitches individual images together once imaging is complete. This removes the need to transfer images to a more powerful computer for stitching as is necessary with CaptuRING. Additionally, both of these systems are designed to capture images along a singular axis as the entire width of a core fits within a single image's field of view. This assumption fundamentally restricts the digitization to be limited only to cores, as cookies have a two dimensional scanning surface.

We made TIM to combine the open-source and open-hardware philosophies of CaptuRING with the functionality of Gigapixel. We added support to digitize both cookies and cores, increased the maximum sample length, perform image stitching directly without the need for manual file transfer, and capture batches of samples sequentially—all while minimizing cost. Our design requires the use of 3D printed components and common hand tools such as allen keys and wrenches. No specialized equipment or power

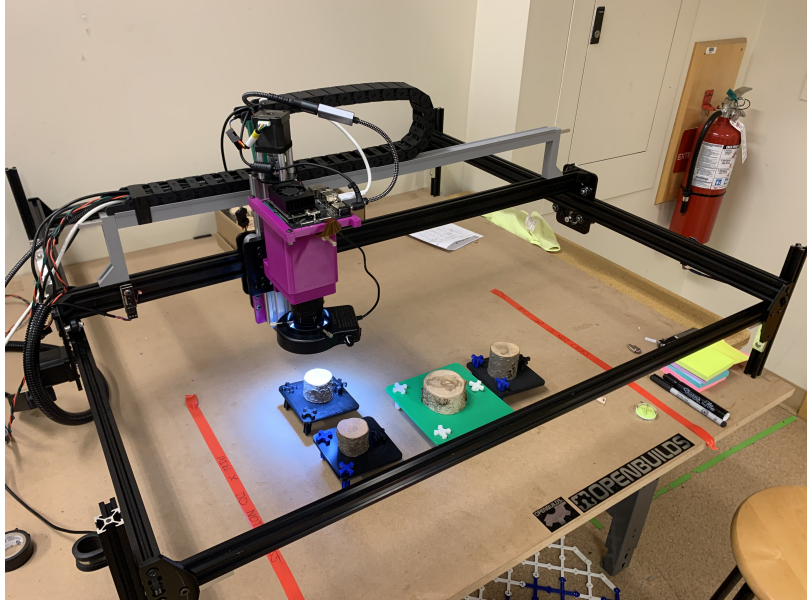


Figure 1: Complete assembly of TIM. Included in the work plane a few cookies ready to be scanned.

tools are required beyond this. Excluding 3D printed parts, the total cost of the machine is approximately \$2 200 USD compared to the \$70 000 USD of the Gigapixel [5]. We chose to use a Raspberry Pi HQ camera with a microscope lens to save on purchasing a professional camera with a macro lens. Professional camera setups are comparable in price to the entire cost of TIM. Additional savings can also be had when factoring in the cost of a professional stitching software license such as PTGui, the suggested software to use with CaptuRING.

2 Methods

2.1 TIM System Design

TIM can be thought of as a combination of multiple subsystems: a gantry machine, camera, and computer (See Figure 1). For the gantry machine, cartesian movement in the X , Y and Z directions is a result of two machine kits and a motor controller from OpenBuilds—the ACRO 1010, the NEMA 17 lead screw linear actuator, and the X32 Motor Controller running GRBL firmware. The machine kit includes extruded aluminum rails, carriages to slide along the rails, stepper motors to control the X and Y movement, and all the hardware to assemble the machine. To fit on the build plates of the ACRO system, we made an adapter to connect the linear actuator to the X and Y axis, thus creating motion in the Z axis. The size of the work plane is ultimately up to the size of the ACRO kit that is purchased—allowing for more flexibility. Building on top of kits allowed for quick assembly with sound instructions and saved development time. For the camera, we chose a 12MP Raspberry Pi HQ Camera equipped with a SEEED studio microscope lens and connected this to the gantry machine using custom adapters. For the computer, we implemented all of the software control, image stitching, and graphical user interface (GUI) to run on an NVIDIA Jetson Orin Nano (Jetson) which also connects to the camera via a MIPI cable. Controlling the machine is done by launching a Python

program and interacting with mouse button clicks on the GUI.

By choosing this combination, we were able to reduce the weight and cost of the camera significantly, which allowed us to invest more in a powerful computer that can handle intensive image processing. The Jetson is an edge computer which drives a monitor for a GUI, sends commands to the motor controller to move the machine, runs image processing calculations for control, and performs calculations to stitch individual images into one mosaic. Despite the weight reductions, torsion on the gantry arm still resulted in a non-zero torsional deflection. A torsion correcting adapter was designed to counteract this rotation and level the lens.

2.2 Preparing Cookies and Cores

TIM can scan both tree cookies and tree cores. Sample preparation for both are equally important but require different approaches. The general guidelines used for preparing cookies and cores applies—requiring samples to be sanded with incrementally increasing sand paper grit to produce an even surface for scanning [20]. We sanded cookies using an orbital sander with mesh sandpaper from 60 to 800 grit, then used a microscope to visually inspect the quality of the sanding. We considered the sample to be sufficiently prepared when vessels were easily identifiable.

Additional sanding considerations need to be taken for each sample type. For cookies, it is important to have the top and bottom surfaces be nearly parallel. Small differences in plane angle can be corrected using the 3D printed levelling table we designed (See Figure 3a). For cores, care should be taken to maximize the scanning surface. This means removing material to be coincident to the center of the cross section of the core. Similarly to cookies, care should be given to achieving a scanning surface as parallel to the XY-plane as possible but generally do not need to be leveled using the levelling tables. Cores also need to be aligned to be parallel to the Y axis to be digitized, using squaring tool or similar to help with alignment. Any warping in core mounts needs to be counteracted with the use of trigger clamps.

2.3 Sample Digitization

The subsystems of TIM can be best understood by following the process from sample setup through obtaining a stitched image. To achieve this with a fixed focus camera, the samples must be nearly orthogonal to the camera lens. Once the sample is level, the operator interacts with the machine through the GUI to navigate the camera to the center of the sample, and focuses the preview image to be sharp by moving in the Z axis. The height and width dimensions are then entered in the GUI to be saved along with the detected center coordinate of the sample. This procedure can be repeated to create a queue of samples to digitize as a batch. The height, width, identifiers, sample type, and centering of the sample is sufficient information to digitize.

2.3.1 Exhaustive Sample Traverse

In the GUI the operator indicates the height and width of the field of view in an individual image from the camera. This varies on the focal length of the lens, but we have kept the field of view to be 3mm x 5mm. Once prompted the system begins to exhaustively traverse the surface area of the sample, using the sample height and width entered by the operator. The goal of this traversal is to obtain in-focus images that have a region

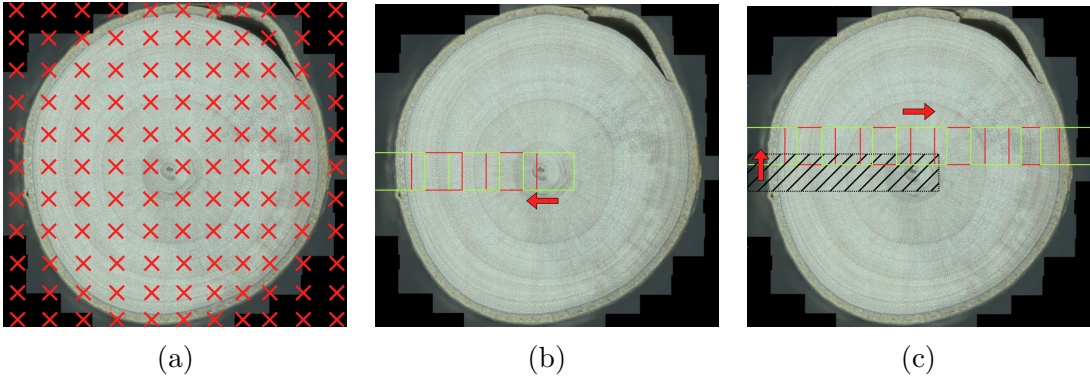


Figure 2: This figure describes the imaging process of a cookie sample after it has been added by a user. In this example, the height and width enclosed the entire surface area of the cookie. (a) A grid of target coordinates is generated to systematically capture partially overlapping images. (b) The first image is taken at the center coordinate of the sample. The rectangular field of view from the camera moves to adjacent target coordinates until it reaches the left boundary—capturing an image for each target coordinate. (c) After completing the row, the machine moves to a new row and continues capturing adjacent images.

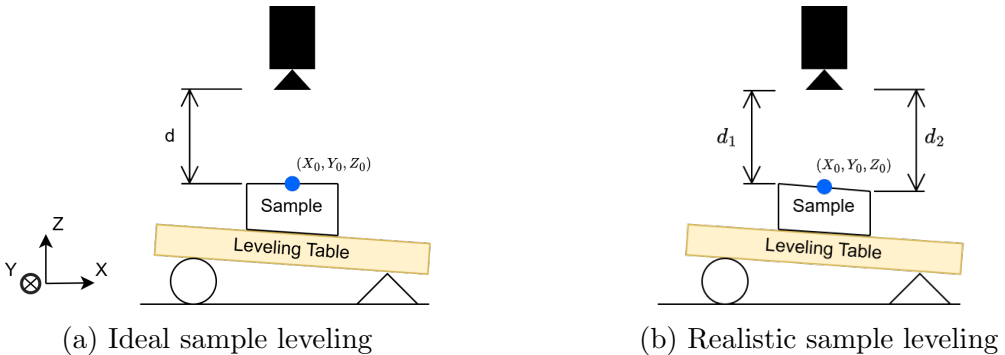


Figure 3: Side view of the camera and sample on top of a leveling table. The ideal sample leveling shows a uniform distance d at all (X, Y) coordinates on the sample. This is impossible to achieve in reality, the true sample leveling has a non-uniform distance at unique (X_i, Y_i) .

of overlap with all its neighbors—the basis of image stitching (See Figure ??). Digitizing cores can be done without needing to traverse in both the X and Y axis. The optimal scanning path for a core is to align the length of cores to the Y axis and only take one column of images. Spanning the surface area of a cookie requires movement in both the X and Y axis.

2.3.2 Image Focusing

Centering the design of TIM around a fixed focus camera and lens means we need to focus the images with a software procedure. The only controllable parameter to focus a fixed focus lens is by changing the lens's distance to the sample. And with the microscope lens, the depth of field of the image is so sensitive that sub millimeter heights can move an image out of focus. Solving this in a time-efficient manner involves two stages. The first stage takes advantage of the requirement to navigate and focus the camera to the center

of the sample. This allows the initial Z_0 value, captured when adding a sample, to be an informed guess as to what value would have an in focus image across the entire surface. From the first (X_0, Y_0) coordinate captured, multiple images are taken at different Z values in $\mathbf{Z}_{samples}$. We found that it is important to have a distance of no more than 0.1 mm between each image in the stack to maximize the likelihood of an in focus image. And with a sufficiently wide height range of 1 mm, we need to take 11 images at different heights for comparison. The number of images taken is an editable parameter in the configuration file and can be increased, along with the height range, if in focus images are not being obtained.

$$Z_{focused} \in \mathbf{Z}_{samples} = Z_0 + \begin{bmatrix} -0.5 \\ -0.4 \\ \vdots \\ 0.4 \\ 0.5 \end{bmatrix}$$

Our focusing procedure begins at 0.5 mm above Z_0 and finishes with the last image at 0.5 mm below Z_0 . The 11 images then have their normalized variance, NV , calculated in a separate thread to measure the image sharpness [12]. The image with the maximum score is saved and can be considered the most in focus image, while the rest are deleted from storage.

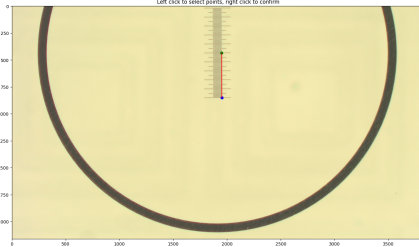
$$i_{max} = \arg \max_i NV(image(\mathbf{Z}_{focus}))$$

The second component of a time-efficient focusing procedure is using a feedback loop to update the initial Z_0 at each image location. Without a feedback loop, the sample alignment must have a difference in height no greater than 0.5 mm, $d_1 - d_2 < 0.5mm$ (See Figure 3b). Rather than adjusting this range, a greater alignment error can be managed by controlling the center of the range, $Z_{0,k}$, for (X_k, Y_k) . The likelihood of an adjacent (X_{k+1}, Y_{k+1}) containing an in focus image is highest when the current $i_{max,k}$ is at the middle index of $\mathbf{Z}_{samples}$. A PID control algorithm with a process variable of i_{max} and control variable of $Z_{0,k}$ allows a negative feedback loop to improve focusing across the entire sample [15]. Instead of forcing a remarkably level sample alignment of $(d_1 - d_2) < 0.5mm$ (See Figure 3b), the system can handle $(Z_k - Z_{k+1} < 0.5mm)$ which is readily achievable.

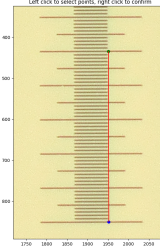
To reduce motion blur in the images, the range of $\mathbf{Z}_{samples}$ is traversed at constant velocity and images are captured without stopping. Decoupling the auxiliary camera control from the G-code commands to control the machine has shown to improve speed and decrease vibrational effects from acceleration and deceleration [16]. This is a variation of the standard approach used in 3D printing and Computer Numerical Control (CNC) machine control.

2.3.3 Accounting for Translation Error Between Core Samples

Difficulties arise when more than one core are added to the digitization queue. The ACRO has a theoretical 4.5 micron translational accuracy, but has not been achieved despite significant effort. These inaccuracies can cause drift in the images with relation to the core and result in the width of the core not being within the field of view of the



(a) Scale Bar for DPI measurements



(b) Zoomed in Scale Bar

Figure 4: Example of a single DPI measurement using a 0.01mm slide scale. The DPI was measured at multiple locations in the field of view both vertically and horizontally. They converged on the same value.

images. We thus implemented a centering procedure that realigns the center of the core to the center of the image frame when the machine moves to a new sample.

First, the camera is moved to the (X_0, Y_0, Z_0) of the new core. From there, the camera is moved across a window, at constant velocity. The width of the window, w in millimeters is defined in the machine configuration file and is editable. $(X_0 - 1/2 * w, Y_0, Z_0)$ to $(X_0 + 1/2 * w, Y_0, Z_0)$. Images are captured at equal distance intervals analogously to the image focusing procedure. Once again, the image with the highest normalized variance score is considered the best image and its location is used as the realigned X'_0 . This procedure drastically improves digitization quality of batches of cores.

2.3.4 Stitching

Image stitching is a well explored field, ranging from panoramic images taken on smart phones to highly tuned microscopy slide stitching. Stitching one image to another requires both to share a region of overlap. When capturing a sample using TIM, the operator has the ability to choose a percentage amount of overlap between images. Most samples are digitized with a percentage overlap between 33% and 50%.

After testing numerous image stitching software APIs, we found the Python package Stitch2D most capable of stitching our images successfully. This package wraps OpenCV functions for finding distinctive image features using the SIFT feature detector and matches these feature within the overlapping region of adjacent images [9]. The default implementation of the package produces high quality stitches but is memory inefficient. We implemented a few key memory conscious changes to the package and were able to run it on the Jetson without a problem.

Some tree ring analyses may not need the maximum scanning resolution produced by TIM. At maximum resolution, TIM's scans quickly produce large file sizes and can be costly to store at scale. To address this, a parameter in the machine configuration file allows the operator to choose a downsizing ratio to apply to images before they get stitched, decreasing the file size of the scans. With the same images, multiple final stitched resolutions can be made.

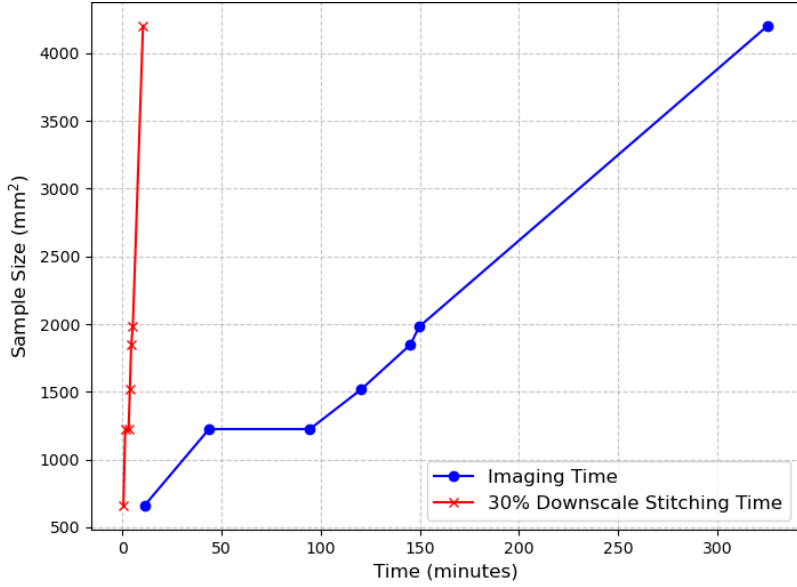


Figure 5: Time to digitize a sample is dependent on the sample’s surface area and the desired final resolution. Cores benefit from linear surface area to sample length. The range of sample included are from a 3mm x 220mm core to a 75mm x 56mm cookie. True sampling times are drastically influenced by configurable machine parameters.

3 Results

TIM is capable of producing extremely high resolution scans. A microscopy slide scale with 0.01mm graduations was used to calculate the dots per inch (DPI) of individual images captured from the system (Figure 4). Using this scale we calculated the maximum DPI to be 21,140. This calculation can be replicated using the Python tool we created as necessary for varied lens focal lengths. When downscaling the final stitch, DPI scales linearly with the downscale percentage defined in the machine parameters.

Digitizing samples takes significantly longer for cookies than it does for cores (Figure 5). This is due to the surface area of cookies requiring more images as it has a square relationship to sample radius. For large cookies, the operator can choose to selectively scan a radius of the cookie instead of the whole surface. A single radius contains a portion of each ring. Scanning complete cookies at maximum DPI is unrealistic as file size limits are quickly encountered with small diameter cookies. To fit into the maximum 2.5 GB limits of a TIFF file, the maximum diameter of a cookie scanned at 30% of maximum resolution is limited to approximately 130 mm. This maximum cookie diameter is significantly smaller than the maximum core sample length. At maximum resolution, the file size limit constrains core samples to approximately 1,500 mm in length. Note that a larger ACRO frame would be needed to support this sample length. Samples that are larger than this file size limit can still be scanned but they are no longer stored as a TIFF file. An uncompressed binary NumPy memory-mapped array file is produced. These NumPy files are not supported by standard image viewers like ImageJ and would require custom tools to work with.

4 Discussion

By taking advantage of a common three degree of freedom cartesian machine design, powerful edge computing, and a microscope camera we were able to design a cost effective and high resolution digitization tool for wood samples. We significantly increased the maximum sample length and maximum resolution compared to common alternatives in the field. In addition, the machine design was intended to be readily replicated by labs with minimal engineering experience and equipment.

4.1 Strengths and Opportunities

Our design minimizes the barriers to build a TIM in smaller labs without compromising scan quality. We have measured tree ring widths using the digitized samples from TIM using CooRecorder as well as ImageJ. Moving forward, TIM could benefit from being integrated into a cloud data storage system with automatic uploads—removing the need to manually transfer completed scans with physical drives. Additionally, developing a framework to run vessel counting or ring identification models while scanning could greatly decrease the time invested in manually identifying tree anatomy.

Our implementation of focusing images could be improved with the aid of additional sensors. Much of the imaging time of samples is the result of taking a vertical stack of images to obtain one in focus image. In advanced microscopy applications, it is common to see supplemental sensors used to measure the distance between the subject and lens. Adding sensor support and a control loop to focus images could significantly reduce sampling time on the scale of an order of magnitude.

References

- [1] Arne Buechling, Patrick H. Martin, and Charles D. Canham. Climate and competition effects on tree growth in Rocky Mountain forests. *Journal of Ecology*, 105(6):1636–1647, 2017. ISSN 1365-2745. doi: 10.1111/1365-2745.12782. URL <https://onlinelibrary.wiley.com/doi/abs/10.1111/1365-2745.12782>. eprint: <https://onlinelibrary.wiley.com/doi/pdf/10.1111/1365-2745.12782>.
- [2] Charles D Canham, Philip T LePage, and K Dave Coates. A neighborhood analysis of canopy tree competition: effects of shading versus crowding. *Canadian Journal of Forest Research*, 34(4):778–787, April 2004. ISSN 0045-5067. doi: 10.1139/x03-232. URL <https://cdnsciencepub.com/doi/abs/10.1139/x03-232>. Publisher: NRC Research Press.
- [3] Harold C. Fritts. Dendroclimatology and dendroecology. *Quaternary Research*, 1(4):419–449, December 1971. ISSN 0033-5894. doi: 10.1016/0033-5894(71)90057-3. URL <https://www.sciencedirect.com/science/article/pii/0033589471900573>.
- [4] Miguel García-Hidalgo, Ángel García-Pedrero, Daniel Colón, Gabriel Sangüesa-Barreda, Ana I. García-Cervigón, Juan López-Molina, Héctor Hernández-Alonso, Vicente Rozas, José Miguel Olano, and Víctor Alonso-Gómez. CaptuRING: A do-it-yourself tool for wood sample digitization. *Methods in Ecology and Evolution*, 13(6):1185–1191, 2022. ISSN 2041-210X. doi: 10.1111/2041-210X.

13847. URL <https://onlinelibrary.wiley.com/doi/abs/10.1111/2041-210X.13847>.
13847. eprint: <https://onlinelibrary.wiley.com/doi/pdf/10.1111/2041-210X.13847>.
- [5] Daniel Griffin, Samantha T. Porter, Matthew L. Trumper, Kate E. Carlson, Daniel J. Crawford, Daniel Schwalen, and Colin H. McFadden. Gigapixel Macro Photography of Tree Rings. *Tree-Ring Research*, 77(2):86–94, July 2021. ISSN 1536-1098, 2162-4585. doi: 10.3959/TRR2021-3. URL <https://bioone.org/journals/tree-ring-research/volume-77/issue-2/TRR2021-3/Gigapixel-Macro-Photography-of-Tree-Rings/10.3959/TRR2021-3.full>. Publisher: Tree-Ring Society.
 - [6] Régent Guay, Réjean Gagnon, and Hubert Morin. A new automatic and interactive tree ring measurement system based on a line scan camera. *The Forestry Chronicle*, 68(1):138–141, February 1992. ISSN 0015-7546, 1499-9315. doi: 10.5558/tfc68138-1. URL <http://pubs.cif-ifc.org/doi/10.5558/tfc68138-1>.
 - [7] Frédéric Guibal and Joël Guiot. Dendrochronology. In Gilles Ramstein, Amaëlle Landais, Nathaelle Bouttes, Pierre Sepulchre, and Aline Govin, editors, *Paleoclimatology*, pages 117–122. Springer International Publishing, Cham, 2021. ISBN 978-3-030-24982-3. doi: 10.1007/978-3-030-24982-3_8. URL https://doi.org/10.1007/978-3-030-24982-3_8.
 - [8] Tom Levanič. Atrics – A New System for Image Acquisition in Dendrochronology. *Tree-Ring Research*, 63(2):117–122, December 2007. ISSN 1536-1098, 2162-4585. doi: 10.3959/1536-1098-63.2.117. URL <https://bioone.org/journals/tree-ring-research/volume-63/issue-2/1536-1098-63.2.117/Atrics--A-New-System-for-Image-Acquisition-in-Dendrochronology/10.3959/1536-1098-63.2.117.full>. Publisher: Tree-Ring Society.
 - [9] David G. Lowe. Distinctive Image Features from Scale-Invariant Keypoints. *International Journal of Computer Vision*, 60(2):91–110, November 2004. ISSN 0920-5691. doi: 10.1023/B:VISI.0000029664.99615.94. URL <http://link.springer.com/10.1023/B:VISI.0000029664.99615.94>.
 - [10] Michael E. Mann, Raymond S. Bradley, and Malcolm K. Hughes. Northern hemisphere temperatures during the past millennium: Inferences, uncertainties, and limitations. *Geophysical Research Letters*, 26(6):759–762, 1999. ISSN 1944-8007. doi: 10.1029/1999GL900070. URL <https://onlinelibrary.wiley.com/doi/abs/10.1029/1999GL900070>. eprint: <https://onlinelibrary.wiley.com/doi/pdf/10.1029/1999GL900070>.
 - [11] Charles W McMillin. Application of Automatic Image Analysis to WoodScience. *Wood Science*, 14(3):97–105, 1982.
 - [12] Hashim Mir, Peter Xu, and Peter Van Beek. An extensive empirical evaluation of focus measures for digital photography. page 90230I, San Francisco, California, USA, March 2014. doi: 10.1117/12.2042350. URL <http://proceedings.spiedigitallibrary.org/proceeding.aspx?doi=10.1117/12.2042350>.
 - [13] Fatemeh Sadat Mohammadi, Hasti Shabani, and Mojtaba Zarei. Fast and robust feature-based stitching algorithm for microscopic images. *Scientific Reports*, 14(1):

- 13304, June 2024. ISSN 2045-2322. doi: 10.1038/s41598-024-61970-y. URL <https://www.nature.com/articles/s41598-024-61970-y>. Publisher: Nature Publishing Group.
- [14] Jeremy L. Muhlich, Yu-An Chen, Clarence Yapp, Douglas Russell, Sandro Santagata, and Peter K. Sorger. Stitching and registering highly multiplexed whole-slide images of tissues and tumors using ASHLAR. *Bioinformatics (Oxford, England)*, 38(19): 4613–4621, September 2022. ISSN 1367-4811. doi: 10.1093/bioinformatics/btac544.
 - [15] Aidan O'Dwyer. A Summary of PI and PID Controller Tuning Rules for Processes with Time Delay. Part 1: PI Controller Tuning Rules. *IFAC Proceedings Volumes*, 33(4):159–164, April 2000. ISSN 1474-6670. doi: 10.1016/S1474-6670(17)38237-X. URL <https://www.sciencedirect.com/science/article/pii/S147466701738237X>.
 - [16] Sarah Propst and Jochen Mueller. Time Code for multifunctional 3D printhead controls. *Nature Communications*, 16(1):1035, January 2025. ISSN 2041-1723. doi: 10.1038/s41467-025-56140-1. URL <https://www.nature.com/articles/s41467-025-56140-1>. Publisher: Nature Publishing Group.
 - [17] Sung-Hyok Ro and Se-Hun Kim. An image stitching algorithm for the mineralogical analysis. *Minerals Engineering*, 169:106968, August 2021. ISSN 0892-6875. doi: 10.1016/j.mineng.2021.106968. URL <https://www.sciencedirect.com/science/article/pii/S0892687521001977>.
 - [18] William J Robinson and Robert Evans. A MICROCOMPUTER -BASED TREE -RING MEASURING SYSTEM. *Tree-Ring Bulletin*, 40, 1980.
 - [19] Paul R. Sheppard. Dendroclimatology: extracting climate from trees. *WIREs Climate Change*, 1(3):343–352, 2010. ISSN 1757-7799. doi: 10.1002/wcc.42. URL <https://onlinelibrary.wiley.com/doi/abs/10.1002/wcc.42>. _eprint: <https://onlinelibrary.wiley.com/doi/pdf/10.1002/wcc.42>.
 - [20] James H. Speer. *Fundamentals of Tree Ring Research*. University of Arizona Press, January 2010. URL https://www.researchgate.net/publication/259466472_Fundamentals_of_Tree_Ring_Research.
 - [21] A. Park Williams, Joel Michaelsen, Steven W. Leavitt, and Christopher J. Still. Using Tree Rings to Predict the Response of Tree Growth to Climate Change in the Continental United States during the Twenty-First Century. December 2010. doi: 10.1175/2010EI362.1. URL <https://journals.ametsoc.org/view/journals/eint/14/19/2010ei362.1.xml>. Section: Earth Interactions.